Drug Design, Development and Therapy Dovepress

Open Access Full Text Article ORIGINAL RESEARCH

Cardiometabolic Modulation by Semaglutide Contributes to Cardioprotection in Rats with Myocardial Infarction

Haihao Yan[1,2], Wenjing Yao[2], Yanhong Li[1], Tianxing Li[3], Kexin Song[1], Pan Yan[4], Yi Dang[2]

[1]Department of Internal Medicine, Graduate School of Hebei Medical University, Shijiazhuang, Hebei, 050017, People's Republic of China; [2]Department of Cardiology Center, Hebei General Hospital, Shijiazhuang, Hebei, 050051, People's Republic of China; [3]Department of Graduate School of Hebei North University, Zhangjiakou, Hebei, 075000, People's Republic of China; [4]Department of Internal Medicine, Yongnian District Traditional Chinese Medicine Hospital, Handan, Hebei, 057150, People's Republic of China

Correspondence: Yi Dang, Department of Cardiology Center, Hebei General Hospital, Shijiazhuang, Hebei, People's Republic of China, Tel +86-0311-85988645, Email dangyiemail@sina.com

Background: Acute myocardial infarction (AMI) is a significant clinical challenge. Semaglutide has therapeutic potential in cardiovascular disease management, but its specific impact and mechanisms in AMI are not fully understood.

Methods: Twenty-four male Sprague-Dawley rats were divided into three groups: control (Control), infarction-only (MI), and semaglutide-treated (SEMA). Weight, blood glucose, and lipid profiles were analyzed. Cardiac function was evaluated via echocardiography. Histopathological assessment and immunohistochemical analysis were performed. Untargeted metabolomic analysis using LC-MS/MS was utilized.

Results: Semaglutide treatment was associated with a reduction in body weight, blood glucose, total cholesterol (TC), and low-density lipoprotein cholesterol (LDL-C), as well as an enhancement in the left ventricular ejection fraction (Control vs MI vs SEMA, 69.13 ±4.30 vs 30.16±3.17 vs 39.81±6.13, $P < 0.05$). It also had a lower collagen volume fraction (3.05 vs 34.05 vs 17.73, $P < 0.05$) and ameliorated the accumulation of glycogen in the myocardium. Metabolomic profiling revealed differentially expressed metabolites between the control/MI and MI/SEMA groups, predominantly within benzenoid, lipid, and organic acid categories. Pathway enrichment analysis highlighted amino sugar and nucleotide sugar metabolism, chlorocyclohexane and chlorobenzene degradation, and phenylalanine, tyrosine, and tryptophan biosynthesis. Random forest analysis identified key metabolites, including downregulated Docusate sodium, 1-(2-Thienyl)-1-heptanone, and Adenylyl-molybdopterin, alongside upregulated Methylenediphosphonic acid, Choline sulfate, and Lactosamine.

Conclusion: Semaglutide significantly ameliorated myocardial fibrosis and metabolic dysregulation in rats post-myocardial infarction. Its mechanism involves modulating glucose metabolism, lipid metabolism, and organic acid metabolism. Targeted metabolites, including Docusate sodium, 1-(2-Thienyl)-1-heptanone, Adenylyl-molybdopterin, Methylenediphosphonic acid, Choline sulfate, and Lactosamine, are implicated in the metabolic reprogramming induced by semaglutide.

Keywords: semaglutide, myocardial infarction, cardiometabolic, untargeted metabolomic analysis, glucagon-like peptide-1 receptor agonists

Introduction

Acute myocardial infarction (AMI) is a common clinical emergency with significant pathophysiological processes involving myocardial cell necrosis, inflammatory responses, fibrosis, and cardiac energy metabolic disorders.[1,2] Heart failure induced by myocardial infarction is an important cause of cardiovascular death in patients.[3] Current treatments include β-blockers, angiotensin II receptor blockers, and angiotensin-converting enzyme (ACE) inhibitors,[4] but the incidence of adverse myocardial remodeling and progression to heart failure after myocardial infarction remains high. Therefore, there is an urgent need to develop new drugs to delay cardiac remodeling after myocardial infarction.

Received: 17 September 2024
Accepted: 19 November 2024
Published: 30 November 2024

The myocardium is a high-workload, high-energy-consuming tissue that requires an ample energy supply. The normal myocardial energy metabolic pathways are highly adaptable, with 40%–60% of energy derived from fatty acid β-oxidation, and 20%–40% from the oxidation of glucose, lactate, and ketone bodies. After myocardial infarction, the increased energy demand of the heart coupled with a reduced blood supply leads to alterations in cardiac metabolic pathways, promoting cardiac remodeling.[5,6] Current research suggests that normalizing the uptake and oxidation of myocardial glucose and fatty acids by modulating downstream metabolic signals can improve adverse remodeling in the ischemic myocardium.[7,8]

Glucagon-like peptide-1 receptor agonists (GLP-1RAs), such as semaglutide, constitute a new class of hypoglycemic drugs that reduce the incidence of cardiovascular adverse events by lowering blood glucose, blood pressure, and lipid levels.[9,10] A proteomic study of mouse ventricles revealed that mitochondria and metabolism are the main targets of short-acting GLP-1RA therapy postinfarction,[11] indicating that GLP-1RA can exert cardioprotective effects through cardiac energy metabolism.

Liquid chromatography–tandem mass spectrometry (LC–MS/MS) offers high sensitivity and specificity, is capable of detecting minor changes in metabolite intensity, and is widely used in metabolomic studies.[12] Previous metabolomics studies have confirmed the cardioprotective effects of semaglutide and changes in metabolic types in mice with heart failure induced by stress load.[13] However, the cardiac metabolic characteristics of rats with myocardial infarction and the mechanisms by which semaglutide regulates metabolic abnormalities postinfarction have not been fully elucidated.

In this study, for the first time, we explored the different metabolic patterns and differentially abundant metabolites in the hearts of rats postmyocardial infarction treated with semaglutide via untargeted metabolomics. By assessing cardiac energy metabolic markers, cardiac function parameters, and histopathological changes in cardiac tissue, we revealed potential targets and pathways involved in the cardioprotection of semaglutide.

Materials and Methods

Animals and Experimental Design

Male Sprague–Dawley rats (300g), purchased from Beijing Weitong Lihua Laboratory Animal Technology Co., Ltd., were housed under conditions of 60% relative humidity, 24°C, and a 12-hour light–dark cycle with ad libitum access to food. The experimental animals were maintained in the Animal Room of the Clinical Medical Research Center, Hebei General Hospital.

After one week of adaptive feeding, the rats were anesthetized via an intraperitoneal injection of 0.3% pentobarbital sodium (1 mL/kg), and myocardial infarction models were established via ligation of the left anterior descending branch. There were 8 rats in each of the control (Control), myocardial infarction (MI), and semaglutide (SEMA) groups. The control group was subjected only to the procedure without ligation. The SEMA group rats were administered semaglutide (0.12 mg/kg/d) subcutaneously 2 hours after myocardial infarction. The control and MI groups were given an equivalent volume of physiological saline subcutaneously; the treatment continued for 4 weeks. Semaglutide was purchased from MedChemExpress and dissolved in pure water for subcutaneous injection. The immediate success of modeling was defined as a change in the color of the myocardium in the left ventricular anterior descending branch supply area from bright red to white, accompanied by ST-segment elevation in the relevant leads of the electrocardiogram. Rat body weight was measured weekly to monitor weight gain. Weigh the feed to calculate the food intake of the rats. Serum and cardiac tissues were collected under anesthesia after 4 weeks of modeling. Serum parameters were measured before the rats were sacrificed. Each repeat was performed as a separate, independent experiment or observation.

Echocardiography

The rats were anesthetized with 0.3% pentobarbital sodium, and depilatory cream was evenly applied to the chest area of each rat. Echocardiographic examination was performed on the rats in each group via a Visual Sonics Vevo 2100 echocardiograph. The left ventricular end-diastolic diameter (LVEDD), left ventricular end-systolic diameter (LVESD), left ventricular end-diastolic volume (LVEDV), left ventricular end-systolic volume (LVESV), left ventricular ejection fraction (LVEF), and left ventricular fractional shortening (LVFS) were measured. The formulas used were LVEDV =

[7.0/(2.4 + LVEDD)] * LVEDD^3, LVESV = [7.0/(2.4 + LVEDS)] * LVEDS^3, LVEF (%) = (LVEDV - LVESV)/LVEDV * 100%. All experiments and data analyses were conducted in a blinded manner to minimize bias.

Detection of Serum Parameters

After fasting for 24 hours, blood was collected from the orbital venous plexus, allowed to stand at 4°C for 30 minutes, and centrifuged at 3500 rpm for 10 minutes. The supernatant was collected into anticoagulant tubes and stored at −80°C. Kits provided by the Institute of Bioengineering in Nanjing, China, were used to measure fasting blood glucose, total serum cholesterol (TC), and low-density lipoprotein cholesterol (LDL-C) levels. The concentration of GLP-1 was detected via an enzyme-linked immunosorbent assay (ELISA).

Histopathological Examination

The chest cavity was opened, and the heart was completely separated. Cardiac tissue from the peri-infarct area of the rat left ventricle was fixed in a 4% paraformaldehyde solution, and the remainder was stored at −80°C.

Cardiac tissue soaked in paraformaldehyde was embedded in paraffin and sectioned (5 μm thick). The tissue sections were stained with hematoxylin and eosin (H&E) and Sirius red. These sections were imaged at 200x magnification in selected tissue target areas under an optical microscope. Sirius red staining was used to assess the collagen content in the myocardial tissue, and the percentage of the collagen area was calculated via the following formula: Collagen area percentage (%) = Collagen pixel area/Tissue pixel area × 100%. Periodic acid-Schiff (PAS) staining was used to detect the accumulation of glycogen in cardiac tissue, which was visualized under an optical microscope at 400x magnification, with glycogen appearing as red particles.

Immunohistochemical Staining

After deparaffinization, the sections were immersed in 3% methanol hydrogen peroxide at room temperature for 20–30 minutes and rinsed with tap water; antigen retrieval was performed at high pressure (95°C), and the sections were blocked with 5% bovine serum albumin for 1 hour. The sections were then incubated with a rabbit anti-GLP-1R antibody (1:200; Proteintech, China) at 4°C overnight. The next day, the sections were washed three times in phosphate-buffered saline (PBS) for 5 minutes each; an HRP-labeled secondary antibody (1:200, Proteintech, China) was applied to the sections, and after incubation at 37°C in the dark for 1 hour, the sections were washed three times in PBS for 5 minutes each; color development was performed via 3.3'-diaminobenzidine, and the integrated optical density was analyzed via Image-Pro Plus software.

Untargeted Metabolomic Analysis

Six samples from each group were randomly selected for untargeted LC–MS/MS analysis. The samples were slowly thawed at 4°C, and an appropriate amount of sample was added to a precooled methanol/acetonitrile/water mixture (2:2:1), homogenized via a homogenizer (60 hz, 15s, 20 times), allowed to stand at −20°C for 1 h, and centrifuged at 14000 × g for 20 min at 4°C, after which the supernatant was used for LC–MS analysis. Metabolomic data were collected via Progenesis QI V2.0 software (Nonlinear, Dynamics, Newcastle, UK).

Further data analysis: Principal component analysis (PCA) was first used to observe the overall distribution of samples and the stability of the entire analysis process. Multivariate statistical analysis was performed via partial least squares discriminant analysis (PLS-DA) and orthogonal partial least squares discriminant analysis (OPLS-DA) to identify overall differences in group metabolic profiles and to screen for differentially abundant metabolites. Differentially expressed metabolites (DEMs) met the criteria of log2FC ≥ 1.0, variable importance in projection (VIP) ≥ 1.0, and $P < 0.05$. Metabolic pathways involving different metabolites were analyzed via the Kyoto Encyclopedia of Genes and Genomes (KEGG) website. In addition, the R package randomForest was used to perform random forest analysis on the metabolomic data, which can determine the importance of metabolites and calculate the mean decrease accuracy (MDA) for each metabolite, with MDA measuring the importance of a metabolite in the metabolic process.

Statistical Analysis

Analysis was performed via the SPSS 26.0 statistical software package. Intergroup comparisons were made via one-way analysis of variance, followed by the least significant difference (LSD) test to determine the statistical significance between groups, with $P < 0.05$ considered statistically significant. All data visualization was performed via GraphPad Prism 9.

Results

Semaglutide Reduces Body Weight, Blood Glucose, and Lipid Levels in Rats with Myocardial Infarction

During the semaglutide intervention period, there was no significant difference in initial body weight between the control and MI groups (Figure 1A). However, after 4 weeks of modeling, there was a statistically significant difference in body weight between the two groups, with the MI group showing a more pronounced increase in body weight. Compared with those of the control and MI groups, the SEMA group presented a slower increase. At the fourth week, the SEMA group had a significantly lower body weight than the control and MI groups did($P < 0.05$). After treatment with semaglutide, starting from the third week, the food intake of rats in the SEMA group was significantly lower than that in the Control and MI groups (Figure 1B). In addition, we assessed TC, LDL-C, and fasting blood glucose levels to evaluate lipid and glucose metabolism in rats with myocardial infarction and the effects of semaglutide. There was no significant difference in the serum TC, LDL-C, or fasting blood glucose levels between the MI and control groups. These indicators were significantly lower after semaglutide intervention ($P < 0.05$) (Figure 1C–E; Supplementary Table S1).

Cardiac Ultrasound Assessment of Cardiac Function

To assess cardiac function, we used several left ventricular (LV) function indices, as shown in Table 1. Four weeks postsurgery, the LVEF and LVFS in the MI and SEMA groups were significantly lower than those in the control group ($P < 0.05$), whereas the LVEDD, LVESD, LVEDV, and LVESV were greater in the MI and SEMA groups than in the

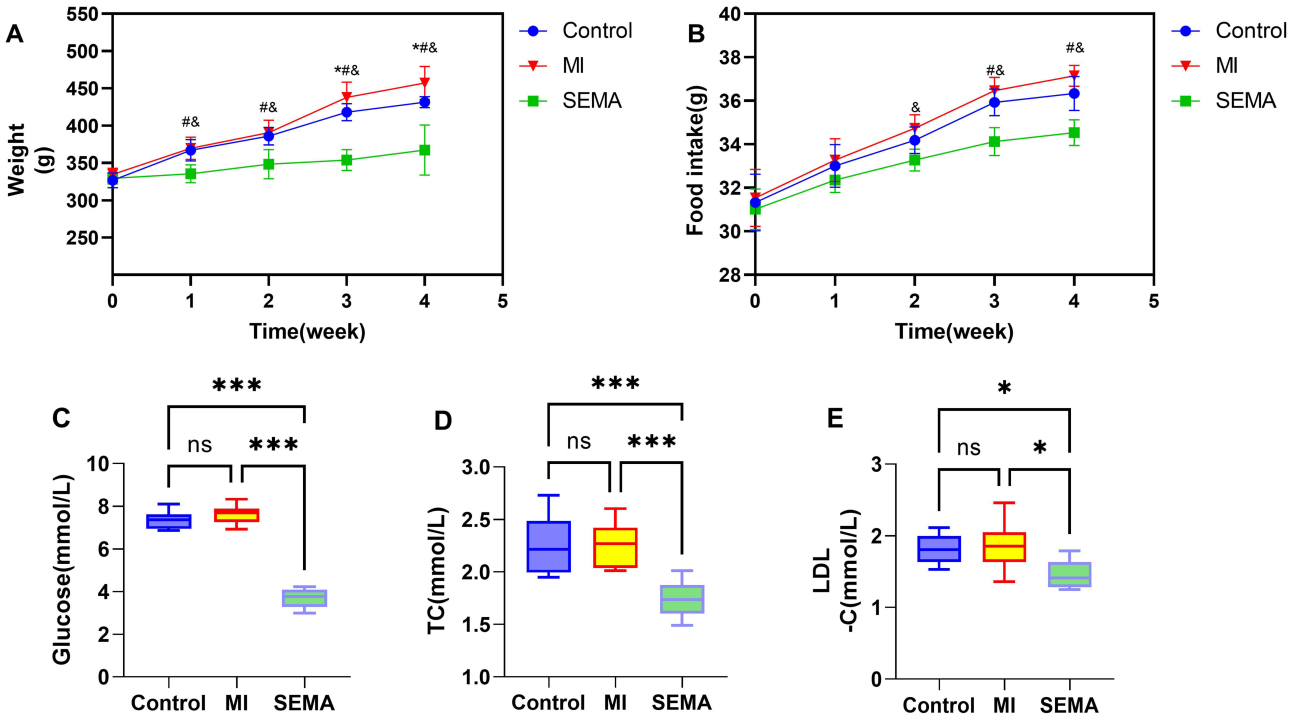

Figure 1 Effects of semaglutide on body weight, blood glucose, and lipid levels in rats with myocardial infarction (n=8), **A–B**: *P < 0.05 indicates control vs MI; #P < 0.05 indicates control vs SEMA; &P < 0.05 indicates MI vs SEMA, **C–E**: *P < 0.05 or ***P < 0.001; ns indicates no statistical significance.

Table 1 Effects of Semaglutide on Cardiac Function in Rats with Myocardial Infarction (n=8)

	Control	MI	SEMA
LVEDD(mm)	5.52±0.98	8.00±0.99*	7.36±0.59*
LVESD(mm)	3.36±0.69	6.81±0.82*	5.89±0.64*#
LVEDV(mL)	0.15±0.06	0.35±0.09*	0.29±0.05*
LVESV(mL)	0.05±0.03	0.24±0.06*	0.17±0.04*#
LVFS(%)	39.30±3.29	14.78±1.76*	20.13±3.51*#
LVEF(%)	69.13±4.30	30.16±3.17*	39.81±6.13*#

Notes: *P < 0.05 compared with the control group and #P < 0.05 compared with the MI group.

control group (P <0.05). Compared with the MI group, the SEMA group presented improvements in LVESD, LVESV, LVFS, and LVEF (P < 0.05).

Serum GLP-1 Detection and Myocardial GLP-1R Immunohistochemistry

The ELISA results revealed that the serum GLP-1 level decreased after myocardial infarction compared with that in the control group, and treatment with semaglutide increased the serum GLP-1 level (P < 0.05). Immunohistochemical results revealed the expression of GLP-1R in the rat myocardium, and after 4 weeks of myocardial infarction, the expression of GLP-1R was significantly lower than that in the sham surgery group. After 4 weeks of treatment with semaglutide, the expression of GLP-1R increased significantly (Figure 2A and B).

Semaglutide Improves Cardiac Remodeling in Rats with Myocardial Infarction

HE Staining: In the control group, the cross-striated muscle structure was relatively intact, with no infiltration of inflammatory cells, and no cellular edema or necrosis was observed. In the MI and SEMA groups, the cross-striated muscle structure was significantly damaged, with a large amount of fibrous tissue proliferation accompanied by cellular edema and necrosis. Compared with the MI group, the SEMA group showed improvement. (Figure 3)

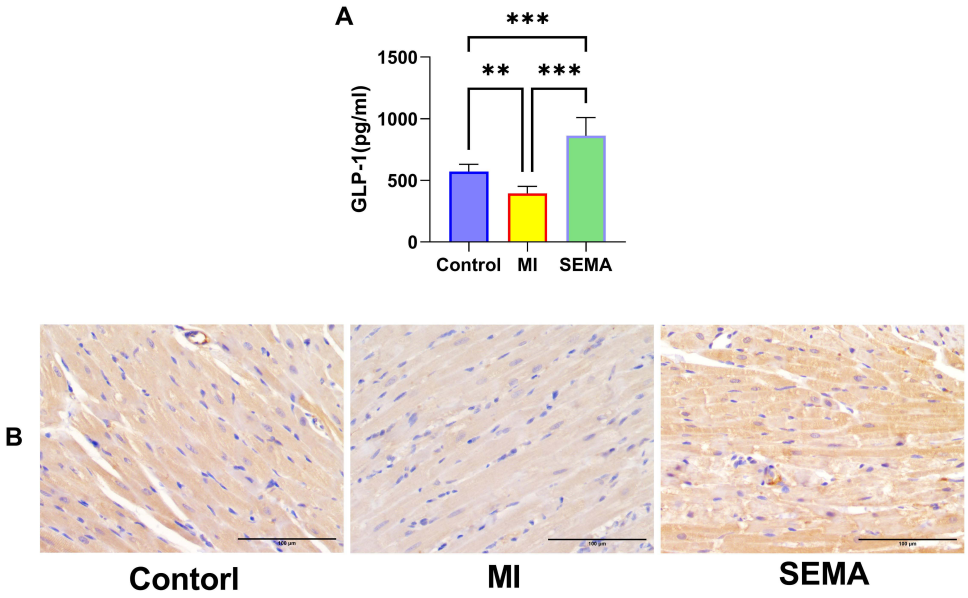

Figure 2 (**A**) Serum GLP-1 detection (n=8), **P < 0.01 or ***P < 0.001. (**B**) Myocardial GLP-1R immunohistochemistry (n=8).

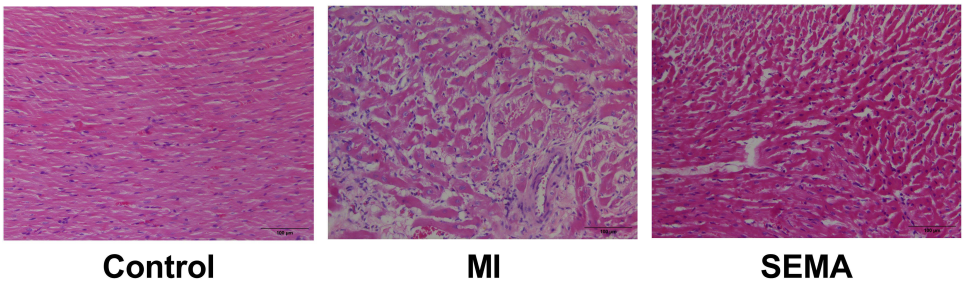

Figure 3 HE Staining (n=8).

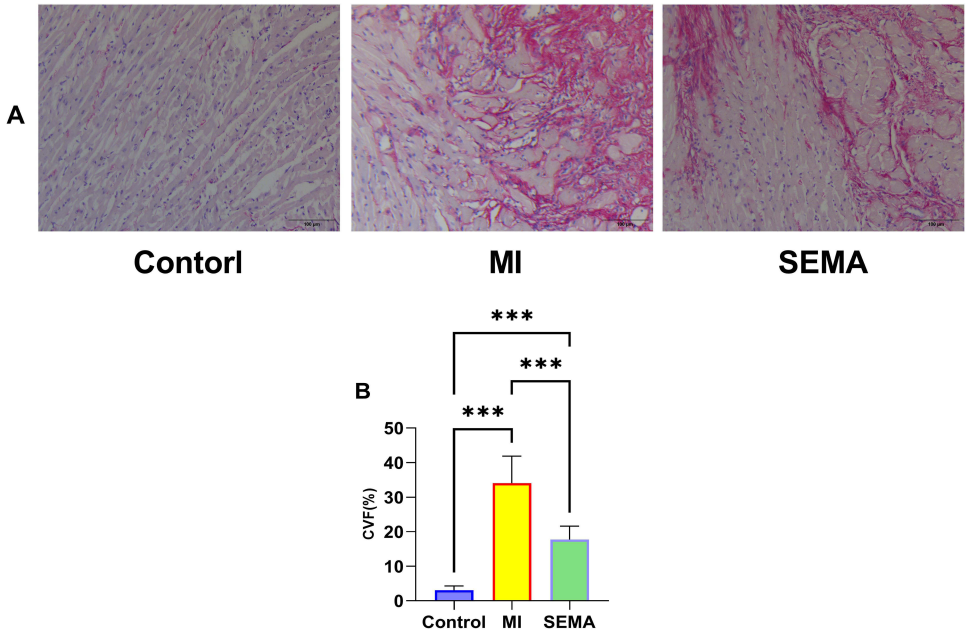

Figure 4 (**A**) Sirius Red Staining (n=8). (**B**) Collagen fiber area (CVF, n=8), ***P < 0.001.

Sirius Red Staining: In the control group, the myocardial tissue was arranged neatly and closely, with a small amount of red collagen deposition visible under the microscope. In the MI group, the muscle fibers were loosely and disorderedly arranged, with many red collagen fibers deposited, and the original fiber structure disappeared. In the SEMA group, the deposition of red collagen fibers was significantly reduced, and the degree of fibrosis was significantly improved. The calculation of the collagen fiber area (CVF) revealed that the collagen fiber area was significantly greater in the MI group than in the control group and significantly lower in the SEMA group than in the MI group ($P < 0.05$). (Figure 4A and B)

Semaglutide Improves Myocardial Glucose Metabolism

PAS staining revealed a large accumulation of red glycogen particles in the myocardium of the MI group, which was partially reduced by semaglutide intervention. These results indicate that under MI conditions, glycometabolism is altered, leading to the accumulation of glycogen in the myocardium, and semaglutide can increase the utilization rate of energy substrates. (Figure 5)

Effects of Semaglutide on Myocardial Metabolomics

PLS-DA Analysis

We performed LC–MS/MS analysis on rat cardiac tissue to observe the effects of semaglutide on cardiac metabolic characteristics. We constructed a PLS-DA model that clearly separated the different comparison groups, revealing

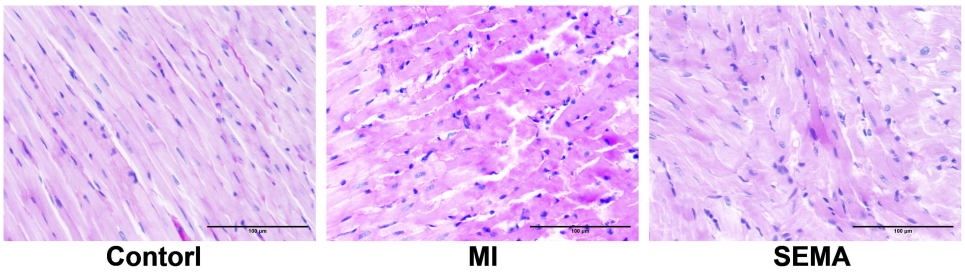

Figure 5 Glycogen Staining (n=8).

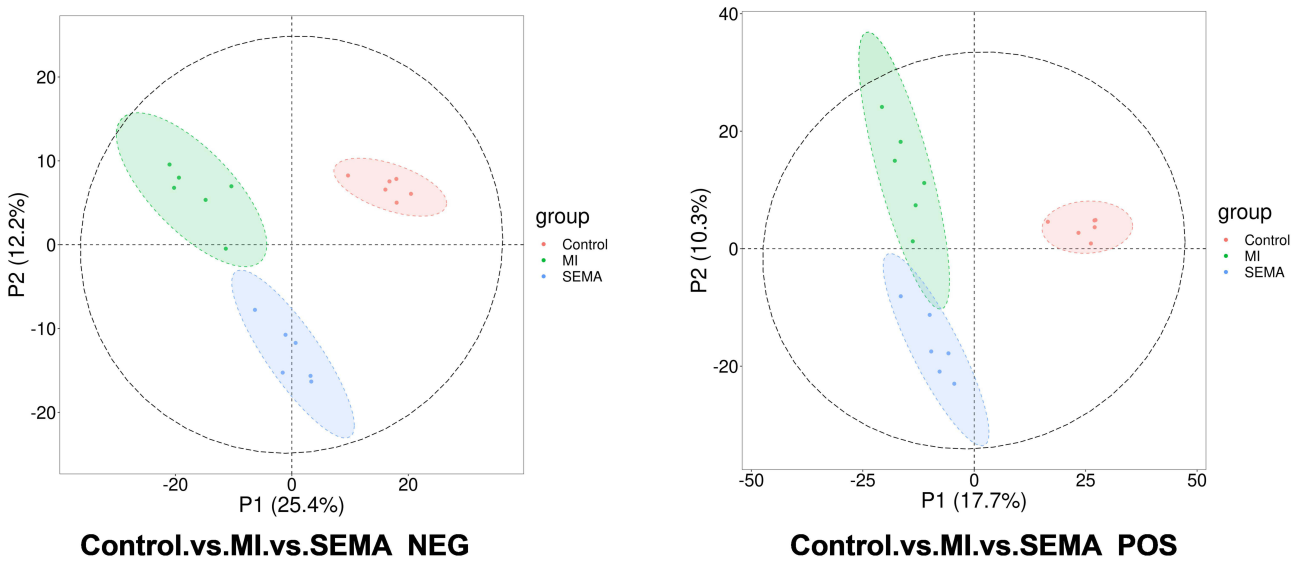

Figure 6 Partial least squares discriminant analysis (PLS-DA) based on the metabolic features of the three groups (n=6).

significant differences between the control, MI, and SEMA groups, with semaglutide significantly altering the metabolic state of the rats with myocardial infarction (Figure 6).

DEMs Between the Two Groups

We screened for DEMs on the basis of the criteria of log2FC≥1.0, VIP≥1.0, and P< 0.05. In the comparison between the control and MI groups, 48 upregulated metabolites and 127 downregulated metabolites were detected in negative ion mode, and 72 upregulated metabolites and 116 downregulated metabolites were detected in positive ion mode. In the comparison between the MI and SEMA groups, 76 upregulated metabolites and 29 downregulated metabolites were detected in the negative ion mode, and 76 upregulated metabolites and 17 downregulated metabolites were detected in the positive ion mode (Figure 7A). The types of significantly changed metabolites identified via chord analysis are shown in the following figures (Figure 7B–E) and are mainly divided into benzenoids, lipids and lipid-like molecules, organic acids and derivatives, organic oxygen compounds, and organoheterocyclic compounds. The heatmap is shown in Figure 7F–I, and the metabolic states of the control, MI, and SEMA groups in both ion modes were distinctly different. (Supplementary Table S2).

KEGG Pathway Analysis

The figure shows the KEGG enrichment information of the DEMs (Figure 8), with the control/MI group enriched mainly in fructose and mannose metabolism, glycolysis/gluconeogenesis, and 19 other signaling pathways, whereas the MI/SEMA group DEMs were enriched mainly in 6 signaling pathways (Supplementary Table S3). All three groups were enriched in amino sugar and nucleotide sugar metabolism; chlorocyclohexane and chlorobenzene degradation; and phenylalanine, tyrosine, and tryptophan biosynthesis.

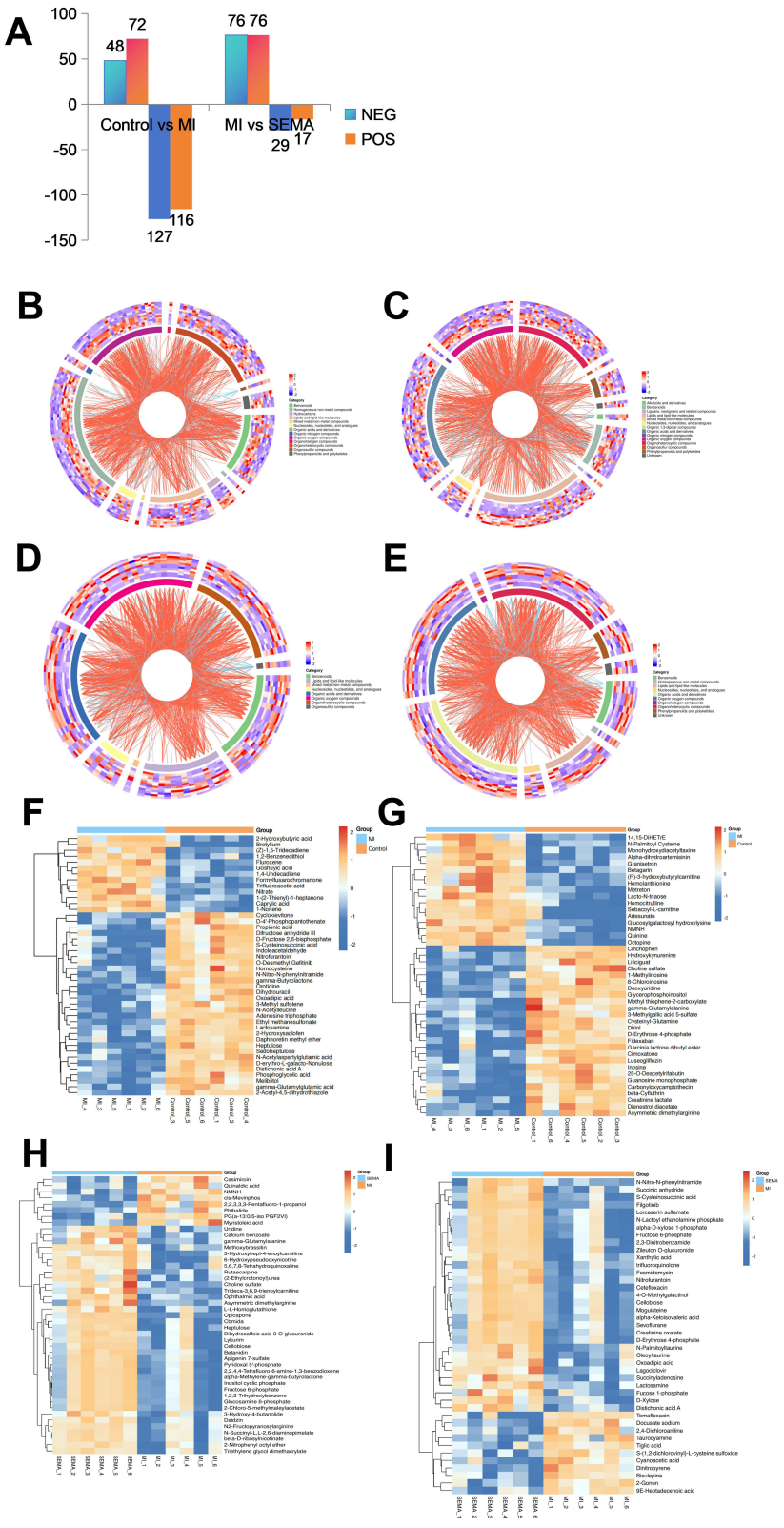

Figure 7 Significantly altered differentially abundant metabolites (DEMs) between the two groups (n=6): (**A**) Number of Increased and Decreased DEMs. (**B**) Chord Analysis of Control vs MI NEG. (**C**) Chord Analysis of Control vs MI POS. (**D**) Chord Analysis of MI vs SEMA NEG. (**E**) Chord Analysis of MI vs SEMA POS. (**F**) Control vs MI NEG. (**G**) Control vs MI POS. (**H**) MI vs SEMA NEG. (**I**) MI vs SEMA POS.

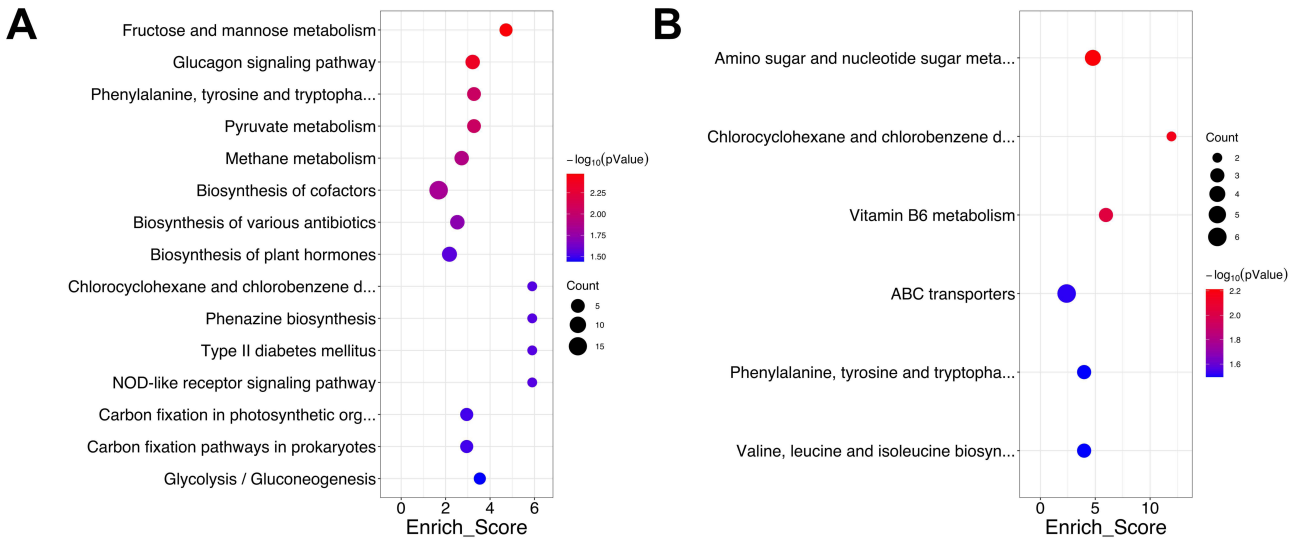

Figure 8 KEGG pathway analysis of the rat DEMs (n=6). (**A**)Control vs MI; (**B**) MI vs SEMA.

Double Volcano Plot for Three-Group Comparisons

We analyzed the common DEMs among the three groups and found that 14 upregulated metabolites in the control/MI group significantly decreased after semaglutide intervention (Figure 9A), whereas 101 downregulated metabolites significantly increased (Figure 9B). These metabolites may be involved in the metabolic regulation of semaglutide in the heart, and some representative common DEMs are marked in the figure (Supplementary Table S4).

Machine Learning: MI Vs SEMA Metabolite Random Forest Plot

We used a random forest to analyze the metabolites of the MI/SEMA group. The horizontal axis on the left side of the figure is the "Mean Decrease Accuracy", which measures the importance of a metabolite in the random forest; the heatmap of the top 15 metabolites in different groups is on the right side (Figure 10A and B). (Supplementary Table S5)

In addition, the top 15 metabolites with MDA values were screened according to previous selection criteria (log2FC ≥ 1.0, VIP≥ 1.0, P< 0.05), and 11 DEMs are listed in Table 2. These molecules have good predictive value for semaglutide intervention in a myocardial infarction rat model. In addition, we combined a double volcano plot to identify 6 biomarkers: semaglutide can reverse the upregulation of Docusate sodium, 1-(2-Thienyl)-1-heptanone, and Adenylyl-molybdopterin induced by myocardial infarction, as well as the downregulation of Methylenediphosphonic acid, Choline sulfate, and Lactosamine to exert cardioprotective effects on rats with myocardial infarction.

Discussion

Cardiovascular diseases are a leading cause of mortality worldwide, with persistently high death rates in recent years. The World Health Organization reports that cardiovascular diseases are responsible for 17 million deaths annually, accounting for approximately 31% of all deaths worldwide, and this number is projected to rise to over 23 million by 2030.[14] Early reperfusion therapies can save lives, but due to ischemia–reperfusion injury and microcirculation disorders, patients still face the risk of complications such as arrhythmias and heart failure, which severely threatens their health and life.[15]

As a new generation of hypoglycemic drugs, GLP-1RAs not only control blood sugar but also achieve weight control.[16] Major studies, such as SUSTAIN6, have confirmed the significant cardiovascular protective effects of GLP-1RAs, which improve the prognosis of patients with cardiovascular diseases.[17–19] A study by Verma confirmed that liraglutide reduced cardiovascular outcomes in patients with a history of myocardial infarction/stroke and in patients diagnosed with atherosclerotic cardiovascular diseases but without a history of myocardial infarction/stroke.[20] Woo and colleagues reported that adjunctive exenatide treatment in patients with ST-segment-elevation myocardial infarction was associated with reduced infarct size and improved left ventricular function.[21] As a highly homologous, novel, long-acting

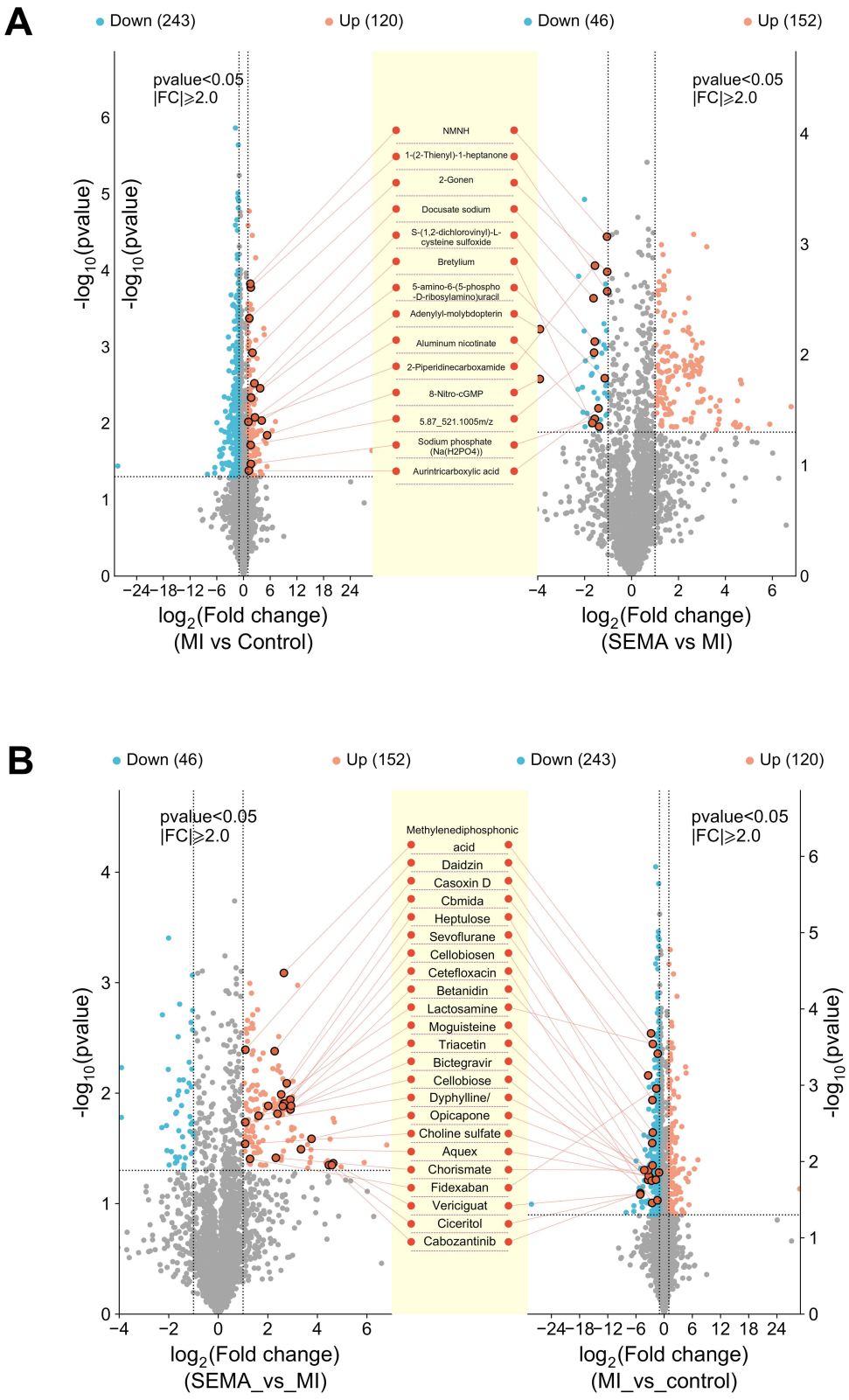

Figure 9 Double volcano plot of the rat DEMs (n=6). (**A**) Common DEMs upregulated in the control/MI group and downregulated in the MI/SEMA group. (**B**) Common DEMs downregulated in the control/MI group and upregulated in the MI/SEMA group.

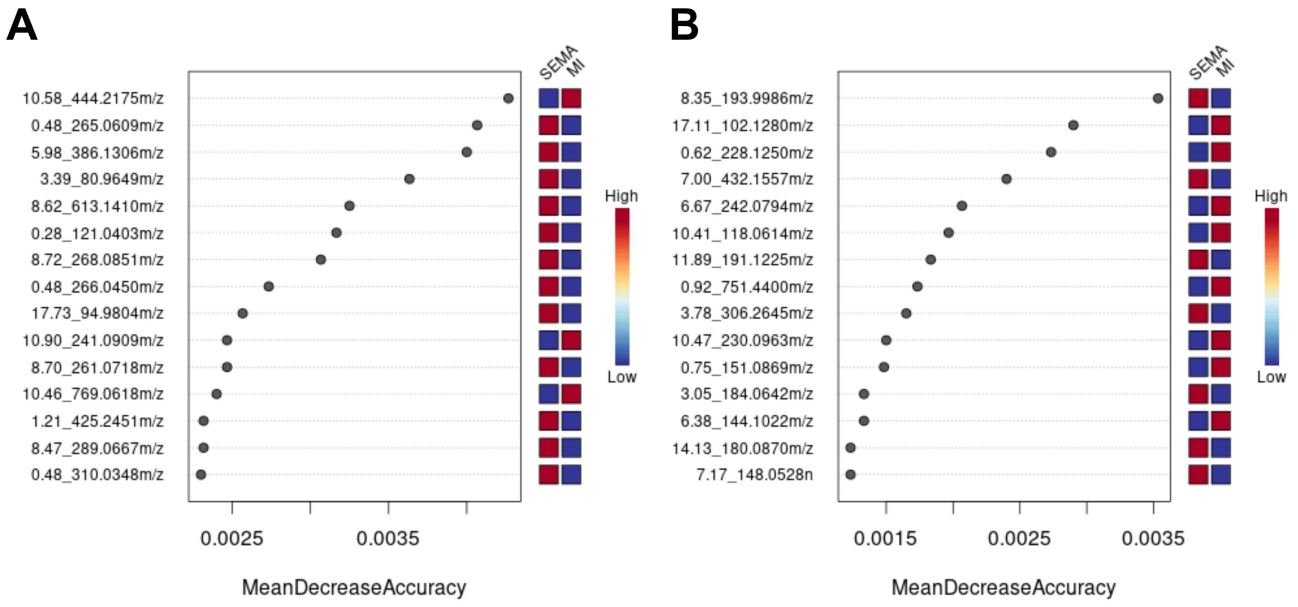

Figure 10 MI vs SEMA random forest plot (n=6). (**A**) MI vs SEMA-NEG random forest plot. (**B**) MI vs SEMA POS random forest plot.

GLP-1RA drug, semaglutide was chosen in this study as the experimental medication for rats with myocardial infarction. After 4 weeks of intervention, the SEMA group had significantly lower body weights than the other two groups did. Additionally, echocardiographic assessments revealed significant improvements in various cardiac function indices, with a notable increase in LVEF, confirming the cardioprotective effects of semaglutide in rats with myocardial infarction. Some studies have shown that elevated GLP-1 levels at admission are closely related to cardiovascular outcomes and complications in patients with myocardial infarction. However, these observational studies do not prove causality. In conjunction with the cardiovascular protective effects of GLP-1, similar to natriuretic peptides, endogenous GLP-1 is

Table 2 Top 15 Metabolites with the Highest Mean Decrease Accuracy (MDA) Values (n=6)

Compound	Formula	Description	VIP	FC	log2FC	pValue	significance	MDA
POS sema vs mi								
8.35_193.9986 m/z	CH6O6P2	Methylenediphosphonic acid	1.43	6.26	2.65	<0.001	Up	0.003533
7.00_432.1557 m/z	C22H23F4NO2	Trifluperidol	1.01	3.00	1.59	0.0018	Up	0.0024
6.67_242.0794 m/z	C7H13O6P	cis-Mevinphos	2.13	0.48	−1.07	0.0061	Down	0.002067
0.92_751.4400 m/z	C37H67O13P	PG(a-13:0/5-iso PGF2VI)	2.11	0.25	−2.01	<0.001	Down	0.001733
3.05_184.0642 m/z	C5H13NO4S	Choline sulfate	2.1	2.12	1.08	0.0288	Up	0.001333
NEG sema vs mi								
10.58_444.2175 m/z	C20H38NaO7S+	Docusate sodium	1.88	0.32	−1.62	0.0031	Down	0.004267
5.98_386.1306 m/z	C12H23NO10	Lactosamine	1.61	4.04	2.02	0.013	Up	0.004
8.72_268.0851 m/z	C10H12FN5O3	Lagociclovir	1.71	3.49	1.80	0.0268	Up	0.003067
10.90_241.0909 m/z	C11H16OS	1-(2-Thienyl)-1-heptanone	1.46	0.49	−1.04	0.0027	Down	0.002467
10.46_769.0618 m/z	C20H26N10O12P2S2	Adenylyl-molybdopterin	1.2	0.07	−3.91	0.0059	Down	0.0024
1.21_425.2451 m/z	C25H34N2O4	Benzeneacetonitrile	1.74	13.31	3.73	0.0382	Up	0.002317

more likely to be a negative feedback in this process, to control glucose metabolism, inflammation, and improve cardiac function during critical illness. Additionally, GLP-1 levels in the short term after onset of the disease do not represent the chronic GLP-1 changes measured in this experiment.[22,23]

Myocardial fibrosis, characterized by excessive proliferation of fibroblasts, is a pathological process that primarily manifests as increased collagen content and disordered arrangement in the myocardial interstitium, leading to reduced myocardial compliance and varying degrees of cardiac dysfunction.[24] In this study, H&E staining revealed that the myocardial structure in both the MI and SEMA groups was significantly damaged, with considerable inflammatory cell infiltration and fibrous tissue proliferation. Compared with the MI group, the SEMA group showed improvements. Sirius red staining revealed a reduction in the collagen fiber area in the SEMA group compared with that in the MI group ($p<0.05$), with a significant improvement in the degree of fibrosis. These findings suggest that SEMA can inhibit myofibroblasts and ameliorate postinfarction myocardial fibrosis in rats.

The heart has a high energy demand and is produced mainly by mitochondrial oxidative phosphorylation to generate ATP to maintain contractile function. Under normal conditions, the energy metabolism pathways of the myocardium exhibit strong adaptability.[6] The reduced metabolic efficiency and loss of coordinated anabolic activities caused by myocardial infarction are significant factors leading to myocardial remodeling. Fatty acids and glucose are the primary "fuels" for generating ATP used in myocardial cell contraction. During cardiac ischemia, the heart can switch from fatty acid oxidation (FAO) to glucose metabolism, enabling the limited oxygen to produce more ATP. This metabolic shift involves increased glucose uptake from the bloodstream, breakdown of cardiac glycogen, reduction of the regulatory enzyme 6-phosphofructokinase-1 (PFK-1) in glycolysis, and activation of AMP-activated protein kinase (AMPK). These changes lead to an increased capacity of GLUT transporters on the membrane and activation of 6-phosphofructokinase-2 (PFK-2).[25] Improving the energy metabolism of the ischemic heart can delay disease progression and reduce infarct size, and it has become a new target in the prognosis and treatment of myocardial infarction. To further clarify the mechanism by which semaglutide affects myocardial metabolism, we conducted metabolomic analysis, examining the DEMs of the Control/MI and MI/SEMA groups, which included mainly benzene compounds, lipids, and organic acids. The metabolic characteristics of the three groups changed significantly. KEGG analysis revealed that the control/MI group was enriched mainly in sugar metabolism, glycolysis, organic synthesis, and amino acid metabolism, whereas the MI/SEMA group was enriched mainly in amino acid metabolism and biosynthesis, as well as sugar metabolism. Glucose metabolism is crucial for improving the function of the infarcted myocardium; a study revealed that reduced cardiac glucose uptake and metabolism in infarcted mice led to a poor prognosis after myocardial infarction.[26] Additionally, our observations indicate that semaglutide has a significant downregulatory effect on blood glucose and blood lipids in rats, and PAS staining also revealed the accumulation of glycogen in the myocardium of the MI group and the increased ability of semaglutide to increase myocardial glucose uptake. Previous studies have confirmed that amino acid metabolism is related to ventricular remodeling in heart failure and the occurrence of CHD.[27,28] Moreover, MI/SEMA also involves valine, leucine, and isoleucine biosynthesis, which, as branched-chain amino acids (BCAAs), play important roles in muscle growth and energy metabolism. Although BCAA oxidation results in less than 2% ATP generation in the heart, the accumulation of BCAAs and branched-chain α-keto acids (BCKAs) has been found in heart failure, mainly because the accumulation of leucine induces the activation of mechanistic target of rapamycin (mTOR) signaling and impairs insulin signaling pathways, leading to ventricular remodeling.[29,30] The common pathways between Control/MI and MI/SEMA include amino sugar and nucleotide sugar metabolism; chlorocyclohexane and chlorobenzene degradation; and phenylalanine, tyrosine, and tryptophan biosynthesis. Among them, amino sugar and nucleotide sugar metabolism is the pathway with the most significant difference between MI and SEMA, and multiple studies have shown its relationship with the regulation of myocardial function, including hypertension, hypertrophic cardiomyopathy, and sepsis-induced myocardial dysfunction.[31–33] These sugars play a key role in the synthesis of complex sugar structures such as glycoproteins, glycolipids, and polysaccharides, and nucleotide sugar metabolism is also involved in the conversion of glucose to ribose, which is essential for nucleic acid synthesis.[34,35] Hyperphenylalaninemia can cause cardiac aging and dysfunction, manifested by increased levels of cytoplasmic superoxide, p21, and H3K9me3 in myocardial cells and/or cardiac fibroblasts, and its mechanism may involve inhibiting the degradation of the p21 protein through targeting its ubiquitination/proteasome-mediated destruction.[36] In addition, cardiac phenylalanine catabolism itself may change

intracellular signal transduction through protein succinylation and aging histone modifications, as well as the accumulation of toxic metabolites, thereby promoting myocardial aging.[37,38] A Mendelian randomization study revealed that tyrosine is positively correlated with angina pectoris and deep vein thrombosis.[39] Tyrosine phosphorylation is an important regulator of cardiac physiology and development, and studies have shown that it affects myocardial tissue structure through the downregulation of the MAPK pathway and the activation of the EGFR, focal adhesion, PDGFR, and actin cytoskeleton pathways.[40,41] In summary, semaglutide regulates glucose metabolism and amino acid metabolism (including BCAA metabolism) and alleviates myocardial injury caused by myocardial infarction through changes in metabolites.

The data collected from untargeted metabolomic analysis are voluminous, necessitating multidimensional spatial modeling of metabolites to facilitate holistic and direct conclusions. The application of machine learning techniques simplifies this process by combining multiple procedures consisting of data resampling and remolding. The random forest method, which involves the construction of an ensemble of decision trees for prediction, can be used in metabolomic research to analyze metabolite data and identify metabolites associated with specific disease states or treatment responses.[42,43] This study is the first to explore biomarkers of drug efficacy in a myocardial infarction model via random forest analysis combined with untargeted metabolomics. We performed a random forest analysis on metabolites from the MI/SEMA group and screened 11 differentially abundant metabolites. We subsequently created a double volcano plot to screen for DEMs reversed by semaglutide intervention. The combination of random forest analysis and the double volcano plot identified common DEMs, including Docusate sodium, 1-(2-Thienyl)-1-heptanone, Adenylyl-molybdopterin, Methylenediphosphonic acid, Choline sulfate, and Lactosamine. Trifluperidol exhibits neuroprotective effects, which may be mediated by modulating inflammatory factors in microglial cells and glial cells. A study suggests that trifluperidol may play a role in regulating glycolysis and cholesterol biosynthesis. It has been described that antipsychotic drugs managed to improve the enzymatic activity associated with the glycolysis pathway.[44,45] Lactosamine is an important endogenous glycoepitope that provides for recognition of glycoproteins by a family of mammalian galectins.[46] The results show that lactosamine is involved in the metabolism of amino sugars and nucleoside sugars, but further mechanism studies are needed. Methylenediphosphonic acid can promote the accumulation of 99Tc-MDP at the site of bone injury, thereby exerting a therapeutic effect. It is reported that 99Tc-MDP can inhibit the expression of bone-destructive factors such as TNF-α, suppress the activity and differentiation of osteoclasts, and improve bone metabolism.[47] These biomarker levels play important roles in the process of glycopeptide intervention and can be further studied in subsequent experiments.

The limitation of this study is the lack of further confirmation via in vitro experiments and comparisons with the efficacy of other drugs, which should be evaluated in future research.

Conclusion

In summary, semaglutide significantly reduces body weight in rats with myocardial infarction, promotes glycolipid metabolism, and markedly improves myocardial fibrosis and metabolic abnormalities. Its mechanism of action may be related to changes in myocardial glucose metabolism and amino acid metabolic pathways, where Docusate sodium, 1-(2-Thienyl)-1-heptanone, Adenylyl-molybdopterin, Methylenediphosphonic acid, Choline sulfate, and Lactosamine play significant roles in metabolic regulation.

List of Abbreviations

AMI, Acute Myocardial Infarction; GLP-1RAs, glucagon-like peptide-1 receptor agonist; LC–MS/MS, liquid chromatography-tandem mass spectrometry; H&E, hematoxylin and eosin; PAS, periodic acid-Schiff; ELISA, enzyme-linked immunosorbent assay; TC, total cholesterol; LDL-C, low-density lipoprotein cholesterol; PBS, phosphate-buffered saline; LVEDD, left ventricular end-diastolic diameter; LVESD, left ventricular end-systolic diameter; LVEDV, left ventricular end-systolic diameter; LVEDV, left ventricular end-diastolic volume; LVESV, left ventricular end-lateral end-systolic volume; LVEF, left ventricular ejection fraction; LVFS, left ventricular fractional shortening; VIP, variable importance in projection; DEMs, differentially expressed metabolites; KEGG, Kyoto Encyclopedia of Genes and Genomes; PLS-DA, partial least squares discriminant analysis; OPLS-DA, orthogonal partial least squares discriminant analysis; PCA, principal component analysis.

Data Sharing Statement

The datasets supporting the conclusions of this article is(are) included within the article (and its additional files).

Ethics Approval and Consent to Participate

Animals used in this study were handled in accordance with the Guide for the Care and Use of Laboratory Animals published by the National Institutes of Health (NIH Publications No. 8023, revised 1978). Animal care and experimental treatment were approved by the animal ethics committee of Hebei General Hospital (NO.202304).

Author Contributions

All authors made a significant contribution to the work reported, whether that is in the conception, study design, execution, acquisition of data, analysis and interpretation, or in all these areas; took part in drafting, revising or critically reviewing the article; gave final approval of the version to be published; have agreed on the journal to which the article has been submitted; and agree to be accountable for all aspects of the work.

Funding

This research received no external funding.

Disclosure

The authors declare that they have no competing interests.

References

1. Reed Grant W, Rossi Jeffrey E, Cannon Christopher P. Acute myocardial infarction. *Lancet*. 2017;389(10065):197–210. doi:10.1016/S0140-6736(16)30677-8
2. Du W, Kangfeng Z, Pengfei H. The role of autophagy in acute myocardial infarction. *Front Pharmacol*. 2019;10:551. doi:10.3389/fphar.2019.00551
3. Virani SS, Alonso A, Benjamin EJ, et al. Heart disease and stroke statistics-2020 update: a report from the American heart association. *Circulation*. 2020;141(9):e139–e596. doi:10.1161/CIR.0000000000000757
4. McMurray JJ, Packer M, Desai AS, et al. Angiotensin-neprilysin inhibition versus enalapril in heart failure. *N Engl J Med*. 2014;371(11):993–1004. doi:10.1056/NEJMoa1409077
5. Gibb Andrew A, Hill Bradford G. Metabolic coordination of physiological and pathological cardiac remodeling. *Circ Res*. 2018;123(1):107–128. doi:10.1161/CIRCRESAHA.118.312017
6. Lopaschuk Gary D, Karwi Qutuba G, Rong T, Wende Adam R, Abel E D. Cardiac energy metabolism in heart failure. *Circ Res*. 2021;128(10):1487–1513. doi:10.1161/CIRCRESAHA.121.318241
7. Yurista Salva R, Herman H W S, Silke U O-M, et al. Sodium-glucose cotransporter 2 inhibition with empagliflozin improves cardiac function in nondiabetic rats with left ventricular dysfunction after myocardial infarction. *Eur J Heart Fail*. 2019;21(7):862–873. doi:10.1002/ejhf.1473
8. Ning L, Masaharu K, Yingchao W, et al. LncRNA LncHrt preserves cardiac metabolic homeostasis and heart function by modulating the LKB1-AMPK signaling pathway. *Basic Res Cardiol*. 2021;116(1):48. doi:10.1007/s00395-021-00887-3
9. Ussher John R, Drucker Daniel J. Glucagon-like peptide 1 receptor agonists: cardiovascular benefits and mechanisms of action. *Nat Rev Cardiol*. 2023;20(7):463–474. doi:10.1038/s41569-023-00849-3
10. Subodh V, Meena B, Melanie D, et al. Effects of once-weekly semaglutide 2.4 mg on C-reactive protein in adults with overweight or obesity (STEP 1, 2, and 3): exploratory analyses of three randomized, double-blind, placebo-controlled, Phase 3 trials. *EClinicalMedicine*. 2023;55:101737. doi:10.1016/j.eclinm.2022.101737
11. de Freitas Germano J, Ankush S, Miroslava S, et al. Proteomics of mouse heart ventricles reveals mitochondria and metabolism as major targets of a post-infarction short-acting GLP1Ra-therapy. *Int J Mol Sci*. 2021;22(16):8711. doi:10.3390/ijms22168711
12. Qingjuan R, Chen S, Chen X, et al. An effective glucagon-like peptide-1 receptor agonists, semaglutide, improves sarcopenic obesity in obese mice by modulating skeletal muscle metabolism. *Drug Des Devel Ther*. 2022;16:3723–3735. doi:10.2147/DDDT.S381546
13. Yu-Lan M, Chun-Yan K, Zhen G, et al. Semaglutide ameliorates cardiac remodeling in male mice by optimizing energy substrate utilization through the Creb5/NR4a1 axis. *Nat Commun*. 2024;15(1):4757. doi:10.1038/s41467-024-48970-2
14. Malakar Arup K, Debashree C, Binata H, Prosenjit P, Arif U, Chakraborty S. Chakraborty Supriyo. A review on coronary artery disease, its risk factors, and therapeutics. *J Cell Physiol*. 2019;234(10):16812–16823. doi:10.1002/jcp.28350
15. Dong Z, Hui W, Liu D, Yun Zhao L, Gang Z. Research progress on the mechanism and treatment of inflammatory response in myocardial ischemia–reperfusion injury. *Heart Surg Forum*. 2022;25(3):E462–E468. doi:10.1532/hsf.4725
16. Christou Georgios A, Niki K, John B, Gema F, Kiortsis Dimitrios N. Semaglutide as a promising antiobesity drug. *Obes Rev*. 2019;20(6):805–815. doi:10.1111/obr.12839
17. Miguel A P-V, Alicia T, Rosa B-LM, García de Lucas María D, Ricardo G-H, Pérez-Belmonte Luis M. Once weekly semaglutide and cardiovascular outcomes in patients with type 2 diabetes and heart failure with reduced left ventricular ejection fraction. *Rev Esp Cardiol (Engl Ed)*. 2024;77(7):583–587. doi:10.1016/j.rec.2023.12.008

18. Mellbin Linda G, Bhatt Deepak L, Jens-Peter D, et al. Semaglutide and cardiovascular outcomes by baseline HbA1c in diabetes: the SUSTAIN 6 and PIONEER 6 trials. *Eur Heart J*. 2024;45(15):1371–1374. doi:10.1093/eurheartj/ehae028
19. Honigberg Michael C, Lee-Shing C, McGuire Darren K, Jorge P, Aroda Vanita R, Muthiah V. Use of glucagon-like peptide-1 receptor agonists in patients with type 2 diabetes and cardiovascular disease: a review. *JAMA Cardiol*. 2020;5(10):1182–1190. doi:10.1001/jamacardio.2020.1966
20. Subodh V, Poulter Neil R, Bhatt Deepak L, et al. Effects of liraglutide on cardiovascular outcomes in patients with type 2 diabetes mellitus with or without history of myocardial infarction or stroke. *Circulation*. 2018;138(25):2884–2894. doi:10.1161/CIRCULATIONAHA.118.034516
21. Jong Shin W, Weon K, Sang Jin H, et al. Cardioprotective effects of exenatide in patients with ST-segment-elevation myocardial infarction undergoing primary percutaneous coronary intervention: results of exenatide myocardial protection in revascularization study. *Arterioscler Thromb Vasc Biol*. 2013;33(9):2252–2260. doi:10.1161/ATVBAHA.113.301586
22. Kahles F, Rückbeil MV, Mertens RW, et al. Glucagon-like peptide 1 levels predict cardiovascular risk in patients with acute myocardial infarction. *Eur Heart J*. 2020;41(7):882–889. doi:10.1093/eurheartj/ehz728
23. Lehrke M, Fuernau G, Jung C, et al. GLP-1 in patients with myocardial infarction complicated by cardiogenic shock-an IABP-SHOCK II-substudy. *Clin Res Cardiol*. 2024;113(8):1211–1218. doi:10.1007/s00392-023-02366-2
24. Navin S, Meijers Wouter C, Silljé Herman HW, de Boer Rudolf A. From inflammation to fibrosis-molecular and cellular mechanisms of myocardial tissue remodeling and perspectives on differential treatment opportunities. *Curr Heart Fail Rep*. 2017;14(4):235–250. doi:10.1007/s11897-017-0343-y
25. Zuurbier Coert J, Luc B, Beauloye Christoph R, et al. Cardiac metabolism as a driver and therapeutic target of myocardial infarction. *J Cell Mol Med*. 2020;24(11):5937–5954. doi:10.1111/jcmm.15180
26. Binsch C, M BD, Hansen-Dille G, et al. Deletion of Tbc1d4/As160 abrogates cardiac glucose uptake and increases myocardial damage after ischemia/reperfusion. *Cardiovasc Diabetol*. 2023;22(1):17. doi:10.1186/s12933-023-01746-2
27. Zhang L, Zhihui, Yanrong Z, Zhong C, Chen Z. Altered amino acid metabolism between coronary heart disease patients with and without type 2 diabetes by quantitative (1)H NMR based metabolomics. *J Pharm Biomed Anal*. 2021. 206: 114381. doi: 10.1016/j.jpba.2021.114381
28. Veera Ganesh Y, Sri Nagarjun B, Harmandeep K, et al. Pressure overload induces ISG15 to facilitate adverse ventricular remodeling and promote heart failure. *J Clin Invest*. 2023;133(9):e161453. doi:10.1172/JCI161453
29. Jinfeng W, Xuefei D, Jiaying C, et al. Metabolic adaptations in pressure overload hypertrophic heart. *Heart Fail Rev*. 2024;29(1):95–111. doi:10.1007/s10741-023-10353-y
30. Wei W, Fuyang Z, Yunlong X, et al. Defective branched chain amino acid catabolism contributes to cardiac dysfunction and remodeling following myocardial infarction. *Am J Physiol Heart Circ Physiol*. 2016;311(5):H1160–H1169. doi:10.1152/ajpheart.00114.2016
31. Xiaonan J, Yahui P, Xiaohui M, Xiaowei L, Kaijiang Y, Changsong W. Analysis of metabolic disturbances attributable to sepsis-induced myocardial dysfunction using metabolomics and transcriptomics techniques. *Front Mol Biosci*. 2022;9:967397. doi:10.3389/fmolb.2022.967397
32. Wen L, Zongkai W, Yanfen Z, et al. Identification of three novel pathogenic mutations in sarcomere genes associated with familial hypertrophic cardiomyopathy based on multiomics study. *Clin Chim Acta*. 2021;520:43–52. doi:10.1016/j.cca.2021.05.034
33. Hao W, Yajun Z, Jing Y, Liping W, Xin Q. Transcriptome and proteome analyses reveal that upregulation of GSTM2 by allisartan improves cardiac remodeling and dysfunction in hypertensive rats. *Exp Ther Med*. 2024;27(5):220. doi:10.3892/etm.2024.12508
34. Gonzalez Grecia M, Svetlana D-M, Hardwick Steven W, et al. Structural insights into RapZ-mediated regulation of bacterial amino-sugar metabolism. *Nucleic Acids Res*. 2017;45(18):10845–10860. doi:10.1093/nar/gkx732
35. Shivani A, Whorton Matthew R. Structural basis for mammalian nucleotide sugar transport. *Elife*. 2019;8:e45221. doi:10.7554/eLife.45221
36. Gabor C, Zaineb M, Altintas Dogus M, et al. Dysregulated phenylalanine catabolism plays a key role in the trajectory of cardiac aging. *Circulation*. 2021;144(7):559–574. doi:10.1161/CIRCULATIONAHA.121.054204
37. Nicola T, Ming Y, Mahima L, et al. Inhibition of mitochondrial aconitase by succination in fumarate hydratase deficiency. *Cell Rep*. 2013;3(3):689–700. doi:10.1016/j.celrep.2013.02.013
38. Andrea Pereira R, Carlos Eduardo Dias J, Tarsila Barros M, Wannmacher Clóvis MD, Dutra Angela DM, Carlos Severo D-F. Phenylpyruvic acid decreases glucose-6-phosphate dehydrogenase activity in rat brain. *Cell Mol Neurobiol*. 2012;32(7):1113–1118. doi:10.1007/s10571-012-9834-2
39. Song H, Zhennan L, Meng-Jin H, et al. Causal relationships of circulating amino acids with cardiovascular disease: a trans-ancestry Mendelian randomization analysis. *J Transl Med*. 2023;21(1):699. doi:10.1186/s12967-023-04580-y
40. Fallou W, Karim B, Coralie P. Protein tyrosine phosphatases in cardiac physiology and pathophysiology. *Heart Fail Rev*. 2018;23(2):261–272. doi:10.1007/s10741-018-9676-1
41. Mingguo X, Bermea Kevin C, Marzieh A, et al. Alteration in tyrosine phosphorylation of cardiac proteome and EGFR pathway contribute to hypertrophic cardiomyopathy. *Commun Biol*. 2022;5(1):1251. doi:10.1038/s42003-022-04021-4
42. Qingyu H, Yuting S, Peihong Y, et al. Quantitative structure-retention relationship for reliable metabolite identification and quantification in metabolomics using ion-pair reversed-phase chromatography coupled with tandem mass spectrometry. *Talanta*. 2022;238(Pt 2):123059. doi:10.1016/j.talanta.2021.123059
43. Marcinkiewicz-Siemion M, Kaminski M, Ciborowski M, et al. Machine-learning facilitates selection of a novel diagnostic panel of metabolites for the detection of heart failure. *Sci Rep*. 2020;10(1):130. doi:10.1038/s41598-019-56889-8
44. Angarita-Rodríguez A, Matiz-González JM, Pinzón A, et al. Enzymatic metabolic switches of astrocyte response to lipotoxicity as potential therapeutic targets for nervous system diseases. *Pharmaceuticals (Basel)*. 2024;17(5):648. doi:10.3390/ph17050648
45. Racki V, Marcelic M, Stimac I, et al. Effects of haloperidol, risperidone, and aripiprazole on the immunometabolic properties of BV-2 microglial cells. *Int J Mol Sci*. 2021;22(9):4399. doi:10.3390/ijms22094399
46. Boscher C, Dennis JW, Nabi IR. Glycosylation, galectins and cellular signaling. *Curr Opin Cell Biol*. 2011;23(4):383–392. doi:10.1016/j.ceb.2011.05.001
47. Mu R, Liang J, Sun L, et al. A randomized multicenter clinical trial of 99 Tc-methylene diphosphonate in treatment of rheumatoid arthritis. *Int J Rheum Dis*. 2018;21(1):161–169. doi:10.1111/1756-185X.12934